The Candidate Sour Taste Receptor, PKD2L1, Is Expressed by Type III Taste Cells in the Mouse

Shinji Kataoka[1,2], Ruibiao Yang[1,3], Yoshiro Ishimaru[4,5], Hiroaki Matsunami[4], Jean Sévigny[6], John C. Kinnamon[1,3] and Thomas E. Finger[1,2]

[1]Rocky Mountain Taste & Smell Center, [2]Department of Cell and Developmental Biology, University of Colorado School of Medicine, Aurora, CO 80045, USA, [3]Department of Biological Sciences, University of Denver, Denver, CO 80208, USA and [4]Molecular Genetics and Microbiology, Duke University, Durham, NC 27710, USA
[5]Present address: Department of Applied Biological Chemistry, Graduate School of Agricultural and Life Sciences, The University of Tokyo, 1-1-1 Yayoi, Bunkyo-ku, Tokyo 113-8657, Japan, [6]Centre de Recherche en Rhumatologie et Immunologie, Centre Hospitalier Universitaire de Québec, Université Laval, Québec, QC, Canada

Correspondence to be sent to: Thomas E. Finger, Department of Cell and Developmental Biology, University of Colorado at Denver and Health Science Center, Mail Stop 8108, P.O. Box 6511, Aurora, CO 80045, USA. e-mail: tom.finger@uchsc.edu

Abstract

The transient receptor potential channel, PKD2L1, is reported to be a candidate receptor for sour taste based on molecular biological and functional studies. Here, we investigated the expression pattern of PKD2L1-immunoreactivity (IR) in taste buds of the mouse. PKD2L1-IR is present in a few elongate cells in each taste bud as reported previously. The PKD2L1-expressing cells are different from those expressing PLCβ2, a marker of Type II cells. Likewise PKD2L1-immunoreactive taste cells do not express ecto-ATPase which marks Type I cells. The PKD2L1-positive cells are immunoreactive for neural cell adhesion molecule, serotonin, PGP-9.5 (ubiquitin carboxy-terminal transferase), and chromogranin A, all of which are present in Type III taste cells. At the ultrastructural level, PKD2L1-immunoreactive cells form synapses onto afferent nerve fibers, another feature of Type III taste cells. These results are consistent with the idea that different taste cells in each taste bud perform distinct functions. We suggest that Type III cells are necessary for transduction and/or transmission of information about "sour", but have little or no role in transmission of taste information of other taste qualities.

Key words: gustation, mouse, polycystic kidney disease–like ion channel (PKD2L1), sour taste, taste bud cells

Introduction

Transient receptor potential (TRP) family ion channels respond to a wide range of extracellular as well as intracellular stimuli. A variety of TRP channels are present in pain fibers and respond to a variety of chemical stimuli ranging from capsaicin to menthol (Voets et al. 2005). One TRP channel, TRPM5 is a crucial element for the transduction of sweet, bitter, and umami tastes. Two TRP channels from the polycystic kidney disease–like (PKDL) family have been implicated in sour taste transduction (Huang et al. 2006; Ishimaru et al. 2006; LopezJimenez et al. 2006).

Taste buds contain numerous elongate receptor cells that detect chemical substances in the oral cavity and transmit this information to the gustatory nerves innervating them. Mammalian taste buds reside in the epithelium of the tongue, palate, pharynx, larynx, and upper esophagus and comprise 4 distinct morphological types of cells (Basal, Type I, Type II, and Type III), which can be identified by distinct ultrastructural and immunohistochemical features (Murray 1973; Takeda and Hoshino 1975; Takeda 1976, 1977; Farbman et al. 1985; Kinnamon et al. 1985, 1988; Delay et al. 1986; Yoshie et al. 1990; Nelson and Finger 1993; Pumplin et al. 1997; Finger and Simon 2000; Yee et al. 2001; Yang et al. 2004; Bartel et al. 2006; Yang et al. 2007). An older classification scheme for taste cells divides the cells according to intensity of cytoplasmic staining into dark, intermediate, and light categories (Finger and Simon 2000). This classification scheme is less useful in that the staining intensity changes according to fixation conditions and other histological factors. Dark cells generally are equivalent to Type I cells, "light cells" to Type II cells, and "intermediate cells" to Type III taste cells.

Type I cells have several long microvilli and many dark granules in the apical cytoplasm. These cells have cytoplasmic processes that envelop nerve fibers and other taste cells, although Type I cells were not observed to have any synaptic contacts (Murray 1973; Pumplin et al. 1997). Type I cells also express neurotransmitter-related enzymes (nucleoside triphosphate diphosphohydrolase 2 [NTPDase2]) and transporters (GLAST) typical of glial cells (Lawton et al. 2000; Bartel et al. 2006). These characteristics of Type I cells suggest a function like glial cells, for example, decreasing neurotransmitter concentration within the extracellular spaces within taste buds.

A Type II cell has several short microvilli of uniform length and a characteristic large, ovoid to round nucleus. These cells display all the components of the taste transduction pathways for sweet, bitter, and umami (taste sensation of glutamate). These cells include T1R or T2R families of taste receptors for umami and sweet (T1R) or bitter (T2R) (Hoon et al. 1999; Zhang et al. 2003) with downstream transduction components, including phospholipase C-β2 (PLCβ2), inositol 1,4,5-triphosphate receptor type 3 (IP$_3$R3) (Clapp et al. 2001; Miyoshi et al. 2001), and transient receptor potential–like channels (TRPM5) (Perez et al. 2002). Many of the T2R-expressing taste cells also express gustducin, the gustatory-related G-protein (McLaughlin et al. 1992; Yang et al. 2000). Type II cells do not have conventional synapses based on ultrastructural criteria. Rather these cells release transmitter in a nonvesicular fashion via pannexin or connexin hemichannels (Huang et al. 2007; Romanov et al. 2007).

A Type III cell has a long microvillus and often forms morphologically identifiable synaptic contacts with the intragemmal nerve fibers. These cells also express immunohistochemical markers such as protein gene–related product 9.5 (PGP-9.5), neural cell adhesion molecule (NCAM) and serotonin (5-HT) (Nelson and Finger 1993; Kim and Roper 1995; Yee et al. 2001). Most recently, Dvoryanchikov et al. (2007) showed that the major catecholamine storage vesicle soluble protein, chromogranin A (CgA), is also present in the Type III taste cells of the mice.

Various mechanisms have been proposed to serve in the detection of sour taste. These include acid-sensing ion channels (ASICs), hyperpolarization-activated cyclic nucleotide–gated (HCN) channels, and 2 pore domain K$^+$ channels (K2P) (Ugawa et al. 1998; Stevens et al. 2001; Ugawa 2003; Lin et al. 2004; Richter et al. 2004a; Richter et al. 2004b). Despite numerous studies, a definitive description of sour receptors and mechanisms remains controversial. Based on molecular biological and functional methods, recent studies have suggested the PKDL ion channel, PKD2L1, and its associated partner PKD1L3, function as a likely candidate for a mammalian sour taste receptor (Huang et al. 2006; Ishimaru et al. 2006). Genetic elimination of cells expressing PKD2L1 substantially reduces neural responses to sour tastants (Huang et al. 2006). These investigators report that PKD2L1 is expressed in a subset of taste cells different from those expressing either T1R or T2R receptors, but it is unclear which taste cell types may express this channel.

To examine the taste cell type expressing PKD2L1, we used double labeling with antibodies directed against NTPDase2 (Bartel et al. 2006) as a marker for Type I cells and PLCβ2 (Clapp et al. 2001; Miyoshi et al. 2001) as a marker for Type II cells. We also used PGP-9.5, NCAM, 5-HT, and CgA as markers for Type III cells. In addition, we used TrpM5-GFP mice (where the TrpM5 promotor and 11 kb of upstream flanking sequence drive GFP expression) to mark Type II cells (Clapp et al. 2006). The goal of the present study is to characterize which types of taste bud cells express this candidate sour receptor. Our results show that PKD2L1 was not present in either Type I or Type II taste bud cells but was coexpressed with each of the Type III markers.

Materials and methods

Immunohistochemistry

The tissues were obtained from C57BL/6J and TrpM5-GFP mice (transgenic line containing 11 kb of mouse TrpM5 5′ flanking sequence, TrpM5 Exon 1 [untranslated], Intron 1, the untranslated part of Exon 2, and eGFP on a C57BL/6J background; Clapp et al. 2006). The University of Colorado Health Science Center Institutional Animal Care and Use Committee approved the procedures and use of animals for these studies. Mice used for 5-HT immunohistochemistry were injected intraperitoneally with 5-hydroxytryptophan (0.08 mg/g; Sigma; St Louis, Mo) 1 h before perfusion (Takeda 1977; Takeda et al. 1981; Yee et al. 2001). After this period, mice were anesthetized with 5% chloral hydrate and perfused transcardially with 4% paraformaldehyde (PFA) in 0.1 M phosphate buffered saline (PBS). After postfixation (1–3 h) and cryoprotection in 30% sucrose in 0.1 M PBS overnight, tissues were sectioned longitudinally or transversely (12 µm) onto Superfrost Plus slides (Fisher Scientific; Hampton, NH).

As for any study utilizing antisera, the tissue staining we report cannot unequivocally be attributed to the presence of the substance against which the antiserum is directed. This study employs only antisera that have been well characterized in the gustatory system by previous investigators. Because of the nature of immunocytochemistry, we refer to the staining we observe as antigen-like immunoreactivity, this terminology conveying the essential uncertainty of an immunocytochemical approach. In all cases, omission of the primary antiserum eliminated the specific pattern of staining that we report.

Double-label staining with PKD2L1 and other taste cell type markers

Staining for NTPDase2 (Bartel et al. 2006; this antibody was raised in rabbit by injection of the complementary DNA, encoding the entire mouse *Entpd2* gene ligated into the

mammalian expression vector), PLCβ2 (Clapp et al. 2001; Miyoshi et al. 2001; rabbit polyclonal antibody raised against a peptide mapping near the C-terminal of PLCβ2 of human origin; sc-206; Santa Cruz, Santa Cruz, CA), Ubiquitin C-terminal hydrolase (PGP-9.5) (Guagliardo and Hill 2007; rabbit polyclonal antibody raised against PGP-9.5 from human brain; 7863-0504; AbD serotec; Raleigh, NC), NCAM (DeFazio et al. 2006; rabbit polyclonal antibody raised against chicken NCAM; AB5032; Chemicon; Temecula, CA), and 5-HT (Huesa et al. 2005; rabbit polyclonal antibody raised against 5-HT coupled to bovine serum albumin with a carbodiimide reaction; 417M; Biomeda; Burlingame, CA) were carried out sequentially because these antibodies were raised in rabbit. The slides were washed 3 times in PBS, followed by 10 min incubation in 0.3% hydrogen peroxide to block endogenous peroxidase activity. After 3 PBS washes, the slides were placed in blocking solution for 1 h. The first rabbit antibody, PKD2L1 (Ishimaru et al. 2006; rabbit polyclonal antibody raised against a peptide corresponding to residue 731–749 of PKD2L1), was diluted in blocking solution (1:7500) and placed on slides overnight. Specificity of the PKD2L1 antiserum was established previously (Ishimaru et al. 2006) by blocking of all immunoreactivity with the cognate peptide. On the next day, slides were washed 3 times in PBS and incubated for 2 h with biotinylated anti-rabbit IgG (1:1000; Vector Laboratories; Burlingame, CA) followed by rinsing in PBS and a 2-h exposure to avidin–biotin complex (PK-6100; Vector Laboratories; Burlingame, CA). After 3 PBS washes, the tissue was reacted with tyramide signal amplification (conjugated to Alexa488; T-20932; Molecular Probes; Eugene, OR) for 7 min before washing slides 4 times in PBS. To ensure that all rabbit IgG–binding sites were blocked, the slides were incubated with unconjugated Fab fragment goat anti-rabbit overnight (1:50 in blocking solution; 111-007-003; Jackson ImmunoResearch Laboratories; West Grove, PA). After 3 rinses in PBS, the slides were placed into blocking solution for 1 h. The second rabbit primary antibodies, NTPDase2 (1:1000), PLCβ2 (1:1000), PGP-9.5 (1:1000), NCAM (1:500), and 5-HT (1:1) were then applied on slides overnight. The slides were washed 3 times in PBS followed by incubation in Alexa568 anti-rabbit (1:400; Molecular Probes; Eugene, OR) for 2 h. After 3 rinses in PBS, the slides were coverslipped with Fluormount G. To ensure the specificity of the second secondary antibody, controls were run in which PKD2L1 was detected as described, but the other primary antiserum was omitted while its secondary (Alexa568 anti-rabbit) was still applied. These sections showed faint diffuse background fluorescence for Alexa568 throughout the epithelium (see Supplementary Figure S1), but this background fluorescence was not localized to particular cells either within the taste bud or in the surrounding epithelium and is thus considered nonspecific background. The specific, well-localized Alexa568 signal we report arose only from binding to the second-applied primary antibodies: NTPDase2, PLCβ2, PGP-9.5, NCAM, and 5-HT. Double-label assays with PKD2L1 and CgA

(1:100 in PBS containing 0.1% Triton X-100 (PBST); Dvoryanchikov et al. 2007; goat polyclonal antibody raised against a peptide mapping at the C-terminal of CgA of human origin; sc-1488; Santa Cruz; Santa Cruz, CA), because the antibodies are derived from separate species (rabbit and goat, respectively), were carried out simultaneously. Elimination of one of the primary antibodies with application of both secondary antibodies confirmed specificity of secondary binding and detection systems. Double immunohistochemistry in fungiform papilla was performed by Zenon labeling kit, as described in the following paragraph. The Zenon labeling kits make it possible to directly label a primary antibody with a tagged Fab fragment prior to application to the tissue section.

Quantification of colocalization

Quantitative analyses were performed from randomly selected fields of the transverse sections in mouse circumvallate. For those analyses, the Zenon rabbit IgG labeling kit (Z-25302, Molecular Probes; Eugene, OR) was used. We used this kit for PLCβ2, PGP-9.5, NCAM, and 5-HT antibodies. The slides were washed 3 times in PBS. After 3 PBS washes, the slides were placed in blocking solution for 20 min. The first rabbit antibody, PKD2L1, was diluted in blocking solution (1:600) and placed on slides overnight. On the next day, slides were washed 3 times in PBS and incubated for 2 h with Alexa568 (1:400). The second rabbit primary antibodies, PLCβ2, PGP-9.5, NCAM, and 5-HT were as in the experiments described above but were prelabeled with corresponding Zenon rabbit IgG Alxa488 for 5 min; the excessive fluorochrome was blocked with blocking agent for another 5 min. During these steps, the antibodies were kept in the dark. For PLCβ2 (1:90), 2 μl of the primary antibody and 2 μl of the Zenon Alexa488 were mixed and incubated for 5 min. Subsequently, 2 μl IgG blocking agent was added and the mixture was incubated for an additional 5 min. Finally, 174 μl PBST was added. For PGP-9.5 (1:60), 2 μl Zenon Alexa488 and 2 μl of the primary antibody were mixed. The mixture was incubated for 5 min. Subsequently, 2 μl blocking agent was added, and the mixture was incubated for 5 min. Finally, 114 μl PBST was added. For NCAM (1:60), 2 μl of the primary antibody and 2 μl of the Zenon Alexa488 were mixed. The mixture was incubated for 5 min after which 2 μl blocking agent was added, and the mixture was incubated for 5 min. Finally, 114 μl PBST was added. For 5-HT (1:10), 3 μl of the primary antibody and 3 μl of the Zenon Alexa488 were mixed. The mixture was incubated for 5 min. Subsequently, 3 μl blocking agent was added and the mixture was incubated for 5 min. Finally, 21 μl PBST was added. The diluted antibodies were brought on to the sections overnight. The slides were performed a second fixation in 4% PFA for 15 min. After 3 rinses in PBS, the slides were coverslipped with Fluormount G. In the Zenon labeling technique, the second-applied primary antiserum

carries with it a direct fluorescent label; hence, it is not possible to perform a specificity control in which the second primary antiserum is omitted because this will also eliminate the second fluorochrome. Instead, specificity is established by the absence of colocalization for some of the antibody combinations but not others. If the Zenon labeling technique were producing artifactual double label, then this artifact would appear similar with all antibody combinations. Such was not the case in our studies.

All images were collected with an Olympus Fluoview confocal laser scanning microscopy using a 60×1.4 numerical aperture objective. Brightness and contrast were adjusted by Adobe Photoshop. For the cell counting, each fluorescence image of double immunohistochemistry was adjusted with manual thresholding, and then we counted identifiable cells of adjusted images with the cell counter plugin for ImageJ (Rasband, W.S., ImageJ, U. S. National Institutes of Health, Bethesda, Maryland, USA, http://rsb.info.nih.gov/ij/, 1997–2007).

Diaminobenzidine electron microscopy

Adult mice were perfused in buffered 4% PFA. After perfusion, the excised circumvallate papillae were fixed in fresh fixative for 3 h at 4 °C. Sections (70 μm thick) were sliced with a vibratome. The free-floating sections were incubated for 1 h in 5% normal goat serum and 3% bovine serum albumin in PBS at 4 °C. The tissue was incubated with anti-PKD2L1 (1:500) antibody overnight at 4 °C. After rinsing in PBS, the sections were incubated with affinity-purified secondary antibody and biotinylated goat anti-rabbit IgG for PKD2L1 in PBS for 2 h at 4 °C. The sections were placed in avidin–biotin complex in PBS for 2 h at 4 °C. Diaminobenzidine (DAB) substrate kit for peroxidase (SK-4100, Vector Laboratories; Burlingame, CA) is used for the DAB staining. After rinsing in PBS, the sections were treated for 10 min in the buffer stock solution containing DAB. The label was visualized for 5 min in a fresh aliquot of the DAB mixture that had been activated with hydrogen peroxide. Sections were washed with 0.05 M Tris buffer and postfixed with 1% OsO_4 in phosphate buffer for 15 min. The sections were washed with 0.05 M sodium maleate buffer (pH 5.2) and then stained en bloc in 1% uranyl acetate in 0.025 M sodium maleate buffer (pH 6.0) overnight at 4 °C. After dehydration in an alcohol series, the sections were processed through propylene oxide and embedded with Eponate 12 (Ted Pella; Redding, CA). The sections were reembedded using the technique of Crowley and Kinnamon (1995). The ultrathin sections were cut with a diamond knife on a Reichert Ultracut E ultramicrotome and examined with a HITACHI H-7000 transmission electron microscopy at 75 kV.

Results

PKD2L1-IR taste bud cells

PKD2L1-IR taste bud cells were slender with a narrow nuclear region, similar in appearance to Type III taste cells but unlike Type II taste cells, which are somewhat broader (Rössler et al. 1998; Clapp et al. 2001; Miyoshi et al. 2001). The PKD2L1-IR cells span the entire height of the taste bud (Figures 1 and 2) with prominent apical processes reaching the taste pore. In particular, the apical region of PKD2L1-IR taste cells displayed intense immunoreactivity (Figure 1B).

PKD2L1 and taste cell types

Type I cells

NTPDase2 is of the predominant ecto-ATPase expressed by Type I taste cells in the fungiform, foliate, and circumvallate papillae (Bartel et al. 2006). Double immunolabeling shows cytoplasmic PKD2L1-IR (Figure 1B) and membrane-associated NTPDase2-IR (Figure 1A) present in separate subsets of taste bud cells of circumvallate papilla. The PKD2L1-IR taste cells do not colocalize with NTPDase2-IR taste cells (Figure 1C).
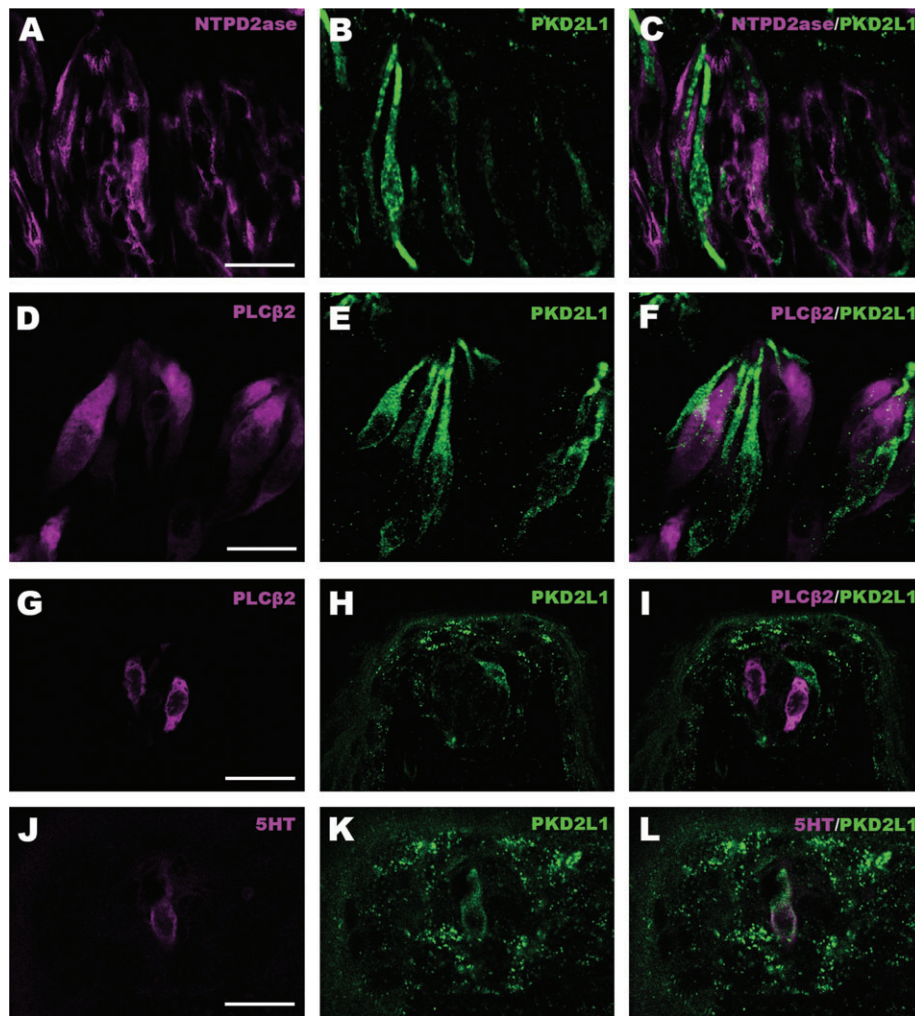
Type II cells

PLCβ2-IR (Figure 1D) is present in taste cells with large, round nuclei, characteristic of Type II cells. Taste cells of circumvallate papilla that display PLCβ2-IR did not frequently express PKD2L1-IR (Figure 1D–F). The PKD2L1-IR cells generally were more narrow than the PLCβ2-IR cells. To test whether PKD2L1-IR taste bud cells even express PLCβ2-IR, we counted immunoreactive cell profiles of cross-sections of taste buds (Figure 3A–C and Table 1). Only 3.4% of the PLCβ2-IR cells expressed PKD2L1, whereas 4.3% of the PKD2L1-IR cells expressed PLCβ2. Cells with detectable coexpression of these substances tended to have relatively faint expression of PKD2L1-IR as shown in Figure 3C (arrow). In the fungiform papilla, no PKD2L1-IR cells were also immunoreactive for PLCβ2, as shown in Figure 1G–I.

In TrpM5-GFP mice, PKD2L1-immunoreactive cells virtually never colocalized with the GFP-expressing population (Figure 4A–C). Because TrpM5 is expressed in Type II cells (Clapp et al. 2006), this further confirms the general absence of PKD2L1 in Type II taste cells.

Type III cells

NCAM-immunoreactive taste cells are Type III cells (Takeda et al. 1992; Nelson and Finger 1993; Yee et al. 2001). Our preparations confirm previous results showing NCAM-IR of membranes of both taste cells and lingual nerves (Figure 2D–F). Over 90% of NCAM expressing cells coexpressed PKD2L1 in circumvallate papilla, whereas 7.1% of NCAM-IR cells did not express PKD2L1 as shown in Figure 3G–I and Table 1.

Injection of the 5-HT precursor 5-hydroxytryptophan results in 5-HT-IR in a subset of Type III cells, as previously described (Takeda 1977; Takeda et al. 1981; Yee et al. 2001). The 5-HT-IR cells are spindle shaped, with an elongate

Figure 1 Confocal laser scanning microscopy images of double-labeled longitudinal sections of **(A–F)** circumvallate taste buds stained for markers of Type I (NTPDase2) and Type II (PLCβ2) taste cells and similar images of **(G–L)** fungiform taste buds showing Type II (PLCβ2) and Type III (5-HT) cells. (A–C) Immu-nofluorescence of NTPDase2 (magenta), PKD2L1 (green), and their overlay. Taste cells positive for NTPDase2 do not show PKD2L1-IR. (D–F) PLCβ2-IR (magenta) and PKD2L1-IR (green) taste cells in 2 taste buds. The PLCβ2-IR cells are different from PKD2L1-IR cells, which tend to be more slender than the PLCβ2-IR cells. (G–I) Taste bud in a fungiform papillae showing lack of colocalization of PLCβ2 (magenta) and PKD2L1 (green). (J–L) Another fungiform taste bud showing double labeling of a taste cell for the Type III marker, 5-HT (magenta) and PKD2L1 (green). Each fungiform taste bud contained only a few cells exhibiting Type III characteristics. Scale bars = 20 μm.

nucleus (Figure 2G) as is typical of Type III cell morphology. Merged images of the 5-HT and PKD2L1 staining confirmed that these 2 substances colocalize in circumvallate papilla (Figure 2G–I and Figure 3J–L). Almost all the 5-HT-IR taste bud cells displayed PKD2L1-IR (Table 1) as evident in Figure 3J–L. In the fungiform papilla, PKD2L1-IR cells also contained 5-HT-IR (Figure 1J–L).

Another marker for Type III taste cells is CgA (Dvoryanchikov et al. 2007). In the present analysis, we found nearly all (93.3%) the PKD2L1-IR cells display CgA LIR (Figures 2J–L and 3M–O and Table 1).

PGP-9.5 immunoreactivity is present in both taste bud cells and nerve processes (Kanazawa and Yoshie 1996; Yee et al. 2001). In rats, PGP-9.5 is expressed in subsets of both Type III and Type II cells. Many cells positive for PGP-9.5 expressed PKD2L1-IR, but not all PGP-9.5–positive cells showed PKD2L1-IR (Figure 2A–C) in circumvallate papilla. In all, 96.7% of the PKD2L1-IR taste bud cells displayed PGP-9.5-IR, whereas 10.3% of PGP-9.5-IR cells did not express PKD2L1 (Figure 3D–F and Table 1).

Quantification of double labeling

We examined the percentage of colocalization between PKD2L1 and Type III cell markers using double-labeling technique. Only 3.4% of PLCβ2-IR taste bud cells (Type II cells) display PKD2L1-IR. In contrast, the PKD2L1-IR taste bud cells nearly completely coexpressed with Type III cell markers. PKD2L1-IR taste bud cells show a high degree of overlap with all Type III markers tested: PGP-9.5 (96.7%), NCAM (96.8%), 5-HT (94.9%), and CgA (93.3%).
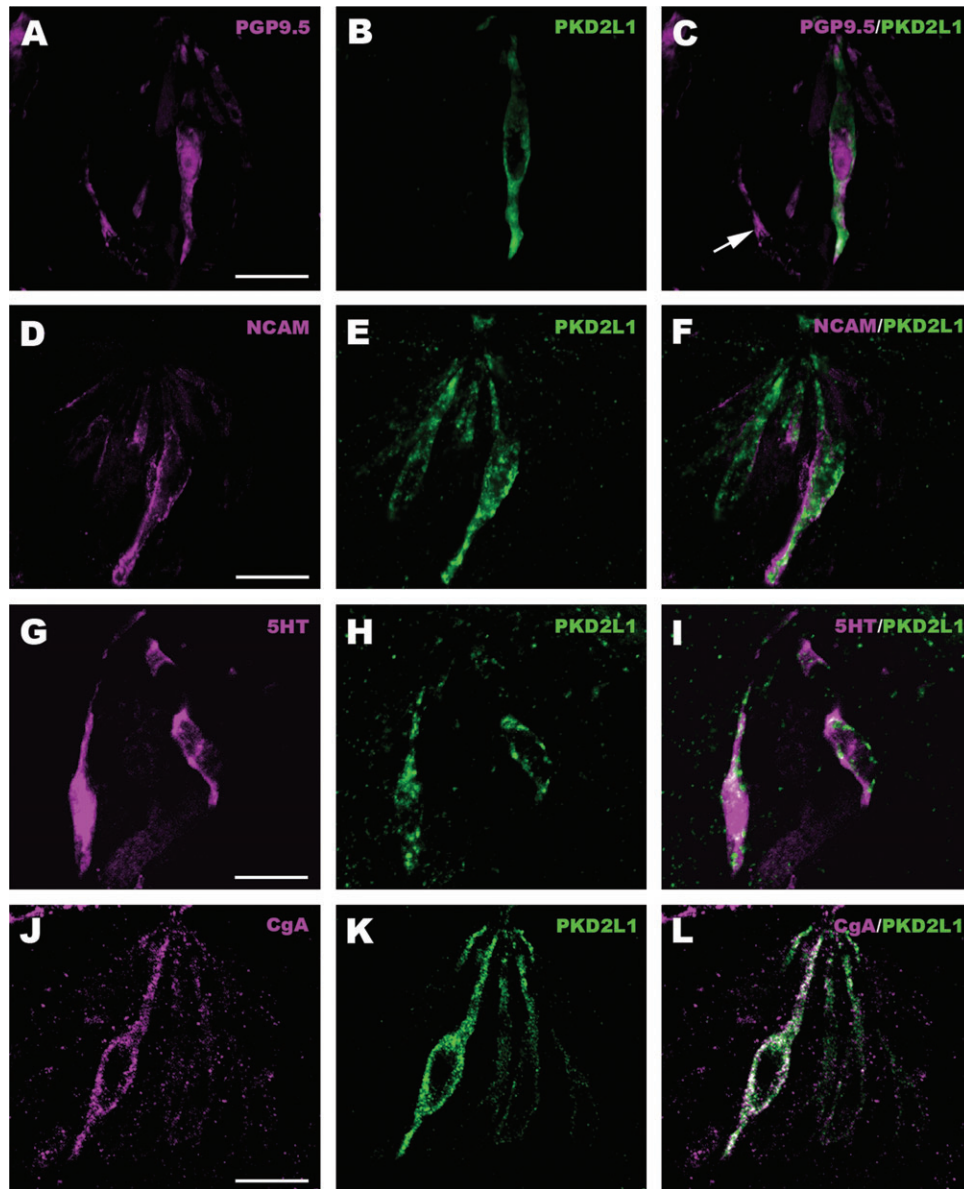
Figure 2 Confocal laser scanning microscopy images of double-labeled longitudinal sections of circumvallate taste buds labeled with markers for Type III taste cells: PGP-9.5 **(A–C)**, NCAM **(D–F)**, 5-HT **(G–I)**, and CgA **(J–L)** along with PKD2L1. (A–C) PKD2L1-IR is present in the PGP-9.5-IR taste bud cells. However, not all cells positive for PGP-9.5 showed PKD2L1-IR (arrow), corresponding to the presence of PGP-9.5 in some Type II cells (Yee et al. 2003). (D–L) PKD2L1-IR colocalizes with markers of Type III cells: (D–F) NCAM-immunoreactive nerve fibers appear as punctate staining between the larger, immunoreactive taste cell profiles. (G–I) 5-HT and (J–L) CgA. Scale bars = 20 μm.

Approximately 10% of PGP-9.5-IR taste bud cells did not express PKD2L1-IR. These taste cells are most probably Type II taste bud cells (Yee et al. 2001). In the fungiform papilla, PKD2L1-IR taste bud cells expressed 5-HT-IR but did not express PLCβ2-IR.

Immunoelectron microscopy

A key feature of Type III taste cells is their unique ability to form "classical" synaptic contacts with nerve fibers complete with presynaptic vesicles and pre- and postsynaptic membrane specializations. In order to assess whether PKD2L1-immunoreactive taste cells possess identifiable synapses, we undertook immunoelectron microscopic investigations. These studies demonstrate numerous examples of synapses between PKD2L1-immunoreactive taste cells and nerve fibers (Figure 5). Both invaginated (Figure 5A,C) and macular (Figure 5B,D) types of synapses were observed.

Panel A is typical of synapses described previously for taste cells; there is modest presynaptic thickening of the membrane with a small number of loosely associated small, clear
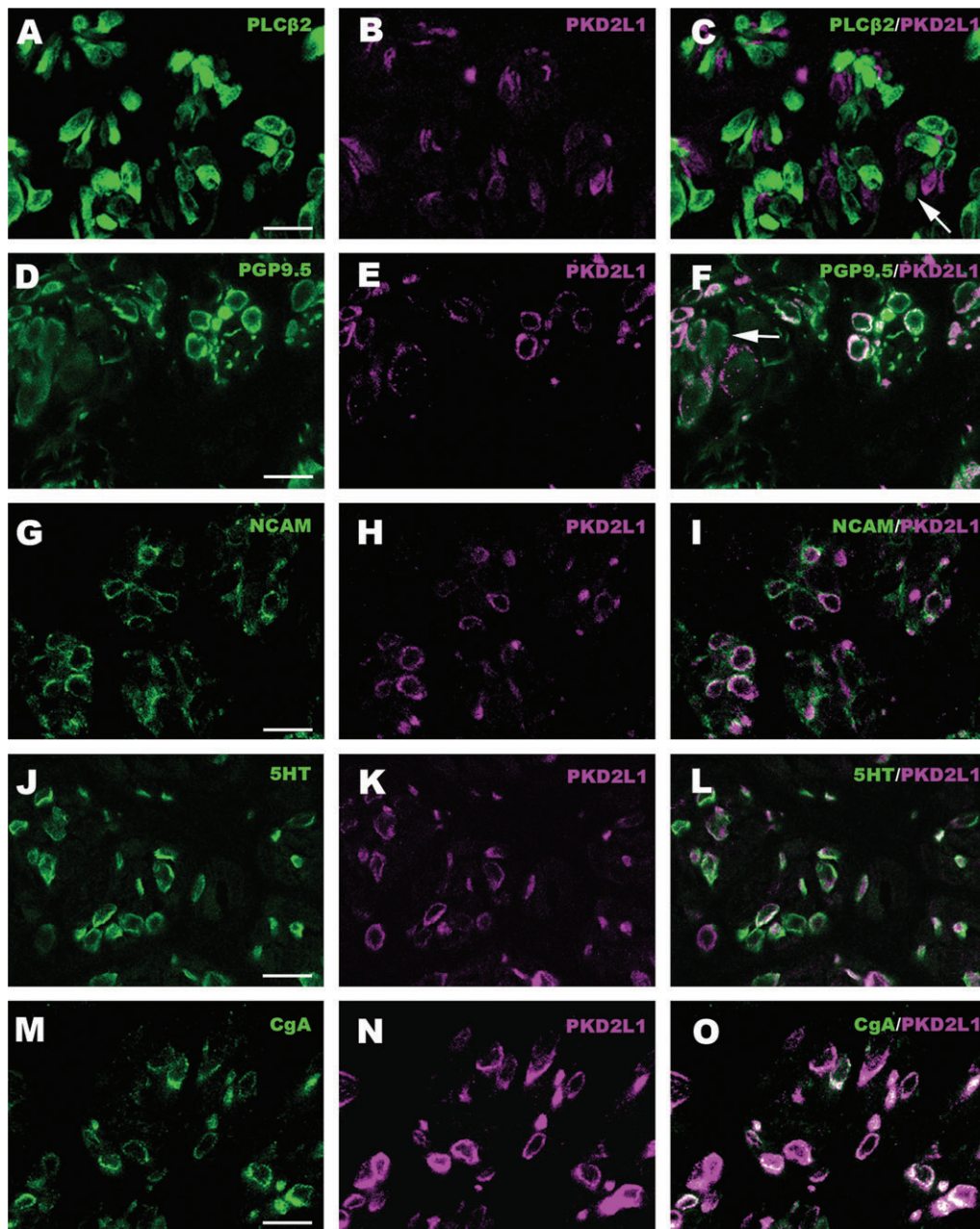
Figure 3   Double-labeled cross-sections through the upper part of circumvallate taste buds showing lack of colocalization of PLCβ2 (Type II cell marker) and PKD2L1 but substantial colocalization with PGP-9.5, which reacts with both Type II and Type III taste cells. Some PGP-9.5-IR cells do not express PKD2L1 (arrow, panel F). The Type III cell markers, NCAM, 5-HT, and CgA essentially completely colocalize with PKD2L1. Green indicates PLCβ2-IR **(A)**, PGP-9.5-IR **(D)**, NCAM-IR **(G)**, 5-HT-IR **(J)**, and CgA-IR **(M)**; and magenta indicates PKD2L1-IR **(B, E, H, K, N)**. Scale bars = 20 μm.

vesicles ranging in size from 40 to 70 nM. A thin postsynaptic membrane thickening is also evident (Figure 5C). Postsynaptic nerve processes often include numerous mitochondria (m in Figure 5B,C).

As summarized in Figure 6, PKD2L1 is expressed by taste cells that exhibit markers of Type III taste cells, including NCAM, PGP-9.5, CgA, and the ability to concentrate amines such as 5-HT. Further, ultrastructural analysis reveals that PKD2L1-immunoreactive taste cells form syn-apses with the intragemmal nerve fibers—a characteristic of Type III taste cells. Few cells with Type II characteristics (e.g., PLCβ2 expression) or Type I characteristics (ecto-ATPase) express PKD2L1.

PKD2L1 in the nonlingual taste buds and solitary chemosensory cells

PKD2L1 was expressed in a subset of taste bud cells in the palate (Figure 4D), pharynx (Figure 4E), and larynx

Table 1 Percent colocalization of various immunocytochemical markers with PKD2L1 in circumvallate taste buds

Immunocytochemical marker	Cell type	Marker—IR taste cells	% Not PKD2L1-IR	PKD2L1-IR Taste Cells	
				Marker—IR taste cells	% Colocalization
PLCβ2	II	116	96.6	93	4.3
PGP-9.5	II and III	128	10.3	120	96.7
NCAM	III	94	7.1	98	96.8
5-HT	III	122	1.5	136	94.9
CgA	III	126	0.8	135	93.3

Cells in 15 taste buds were counted. Taste cells immunoreactive for each marker were identified and then checked for immunoreactivity for the PKD2L1. Cells were scored as positive if they exhibited obvious fluorescence above background levels of reactivity.
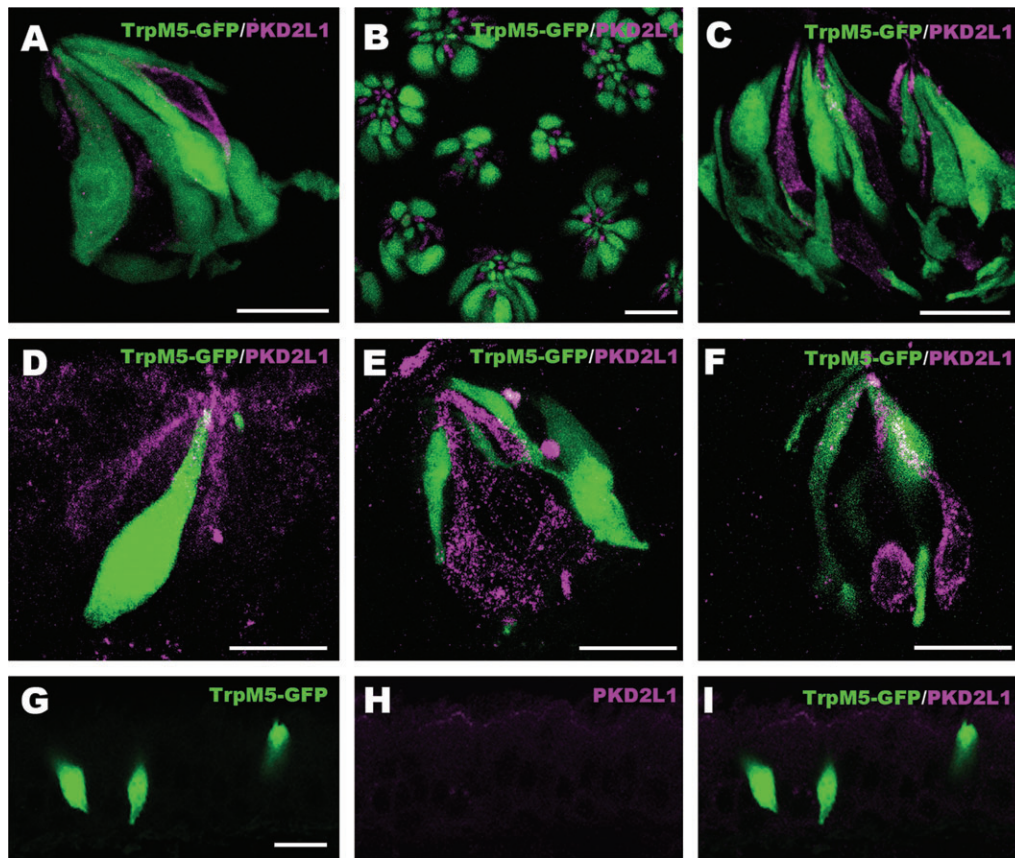

Figure 4 Dual label images showing PKD2L1 (magenta) and GFP as expressed in TrpM5-GFP mice. **(A–C)** These confocal laser scanning microscopy overlay images shows that taste cells positive for PKD2L1 do not express TrpM5 in longitudinal (A) and cross (B) sections of circumvallate, and foliate (C) taste buds. **(D–F)** Expression of PKD2L1 in nonlingual taste buds. These images show that PKD2L1 is present in palate (D), pharynx (E), and larynx (F) taste buds. PKD2L1-expressing taste cells are different from those expressing TrpM5. **(G–I)** Laryngeal solitary chemoreceptor cells are shown (green) in TrpM5-GFP mice. PKD2L1-IR is not detectable in these solitary chemoreceptor cells of the larynx. Scale bars = 20 μm.

(Figure 4F). In TrpM5-GFP mice, PKD2L1 expression in taste cells did not coincide with the green fluorescence of TrpM5-GFP, which marks Type II taste cells (Figure 4A–F). Solitary chemosensory cells identified in larynx by TrpM5-GFP also did not express PKD2L1 (Figure 4G–I).

Discussion

Previous investigators reported that a candidate sour receptor, PKD2L1, is expressed in a subset of taste cells different from those expressing receptors for sweet and umami (T1R), or bitter (T2R) (LopezJimenz et al. 2006; Ishimaru et al.
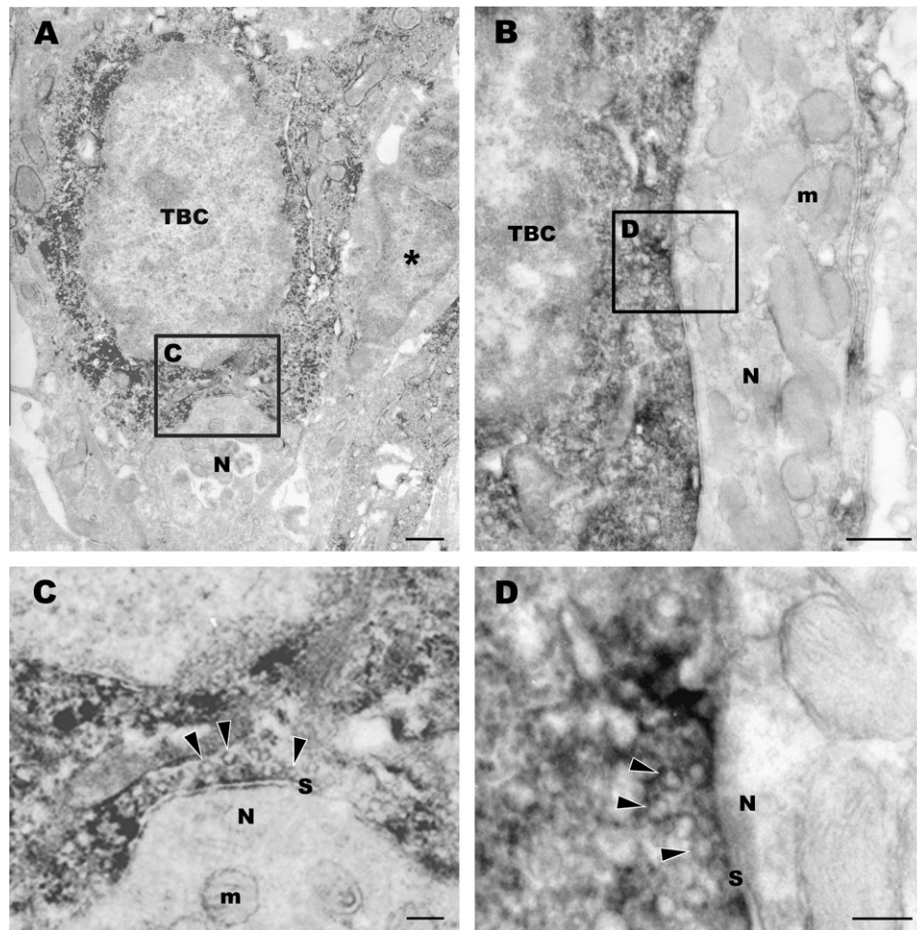
Figure 5 DAB immunoelectron micrograph of taste buds in the circumvallate papilla showing PKD2L1-IR taste bud cells (TBC) with 2 structural types of synapses onto sensory nerve processes. Synapses between taste cells and nerve processes are a characteristic of Type III taste cells. **(A)** A Synapse onto a nerve process (N) indented into the soma of the taste cell is associated with PKD2L1-IR taste bud cell. An adjacent taste bud cell (*) lacks PKD2L1-IR. **(B)** A macular synapse from a taste bud cell with PKD2L1-IR onto a nerve process (N). Numerous mitochondria (m) are present in the postsynaptic process. **(C)** High magnification of boxed area in (A) showing synapse (S). Many synaptic vesicles (arrow heads) are evident in the cytoplasm opposite the point of contact with the nerve fiber. Some mitochondria (m) are also present in the postsynaptic region. **(D)** High magnification of boxed area in (B) showing synapse (S). The PKD2L1-IR taste bud cell contains many clear synaptic vesicles (arrow heads) in the presynaptic region. Scale bars = 1 μm in (A and B); 0.25 μm in (C and D).

2006; Huang et al. 2006) or TrpM5 (Huang et al. 2006; Ishimaru et al. 2006). However it was unclear whether PKD2L1 expression coincides with a specific cell type, and if so, whether it was expressed by an unusual population of Type II taste cells which hitherto have been described as taste receptor cells in contrast to integrative or glial-like cells of the taste bud (DeFazio et al. 2006). PLCβ2, IP$_3$R3, and TrpM5 are present in virtually all Type II taste cells (Clapp et al. 2001; Perez et al. 2002), so it seemed unlikely that PKD2L1 would be expressed by this cell population. Remaining unclear, however, was the nature of the PKD2L1-expressing cells. To address this question, double immunolabeling was performed on mice. In the present study, we showed that PKD2L1 colocalized with all markers of Type III taste cells but not with either Type I or Type II markers, strongly suggesting that PKD2L1 is expressed by the Type III cells. In addition, PKD2L1-immunoreactive taste cells form synapses with the

afferent nerves, further supporting the identity of these cells as Type III taste cells.

Haung et al. (2006) engineered transgenic mice in which PKD2L1 promoter indirectly drove expression of a diphtheria toxin subunit. In these mice, over 95% of PKD2L1-expressing taste cells were ablated, and these mice showed a marked and specific loss of sour taste, including severely reduced neural response to citric acid, acetic acid, and hydrochloric acid (Huang et al. 2006). Our study suggests that elimination of PKD2L1-expressing cells should result in the elimination of the vast majority, if not all, of Type III cells. This has important implications for understanding the cell biological organization of taste buds. First, Type III cells (previously termed "intermediate cells") have been suggested to be crucial precursors to the formation of Type II cells (so-called light cells) (Delay et al. 1986; Miura et al. 2005). If Type III cells are an obligatory maturational step
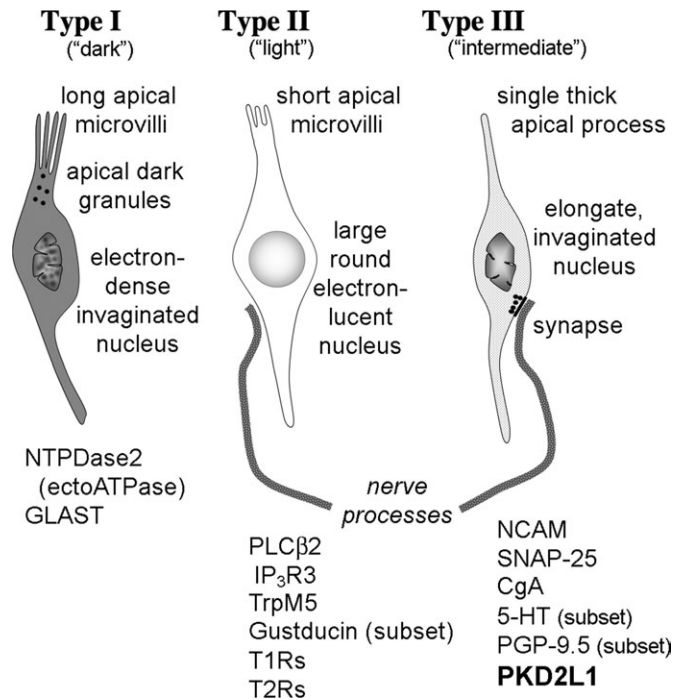
Figure 6 Semischematic diagram showing the main characteristics of the different elongate taste cell types. Not illustrated are Type IV basal cells. Type I taste cells (also called "dark" cells) have several glial characteristics including expression of GLAST and NTPDase2, both features of central glia. Type II cells (also termed "light" or "receptor" cells) express the G-protein–coupled taste receptors (T1R and T2R families) and associated downstream signaling molecules: PLCβ2, IP$_3$R3, TrpM5, and gustducin (in a subset of Type II cells). The Type III cells (also called "intermediate" or "presynaptic" cells [Roper 2006]) form synaptic contacts with nerve fibers and express features of aminergic neurons, including expression of NCAM, SNAP-25, CgA, and the ability to concentrate amines, for example, 5-HT. PKD2L1 is expressed by taste cells that exhibit these features of Type III taste cells.

en route to Type II cell formation, then elimination of Type III cells should also eliminate any Type II cells resulting from a Type III cell lineage. Because Type II cells (those expressing T1Rs and T2Rs) remain following elimination of Type III cells, Type III cells cannot be obligatory progenitors of Type II cells.

Type III cells are the only type of taste cell that exhibit morphologically discernable classical synapses (Murray 1973, 1986; Kinnamon et al. 1985). Accordingly, several investigators suggest that they are the principal means of transmission of taste information to the gustatory nerves (e.g., Kaya et al. 2004; DeFazio et al. 2006; Roper 2006). In other words, stimulation of Type II cells by tastants is hypothesized to release a substance that activates Type III cells, which then synapse with the gustatory nerves. Because genetic ablation of Type III cells does not disrupt communication of bitter, sweet, and umami taste information from Type II receptor cells to the afferent nerves then Type III cells are not obligatory intermediates in this system. Despite lacking classical synapses, Type II cells release neurotransmitter, including ATP, via hemichannels on their basolateral membranes (Romanov

et al. 2007; Huang et al. 2007). The released ATP appears to act directly on P2X receptors on the afferent nerve fibers to convey the gustatory message (Finger et al. 2005). Indeed, genetic elimination of the neural P2X receptors (P2X2 and P2X3) essentially eliminates all neural responses to tastants including sour. Our results taken with those of Haung et al. (2006) demonstrate that Type III cells are not necessary for communication of taste information to the gustatory nerves.

The genetic ablation of PKD2L1-expressing cells in taste buds has been interpreted as strong support for the role of this channel in sour transduction. Yet, the possibility exists that other channels and receptors may contribute to detection of acids by taste buds. The functional candidate sour taste receptor comprises 2 subunits: PKD2L1 and PKD1L3 (Ishimaru et al. 2006). Although taste buds in fungiform papillae give robust responses to sour tastants (Ninomiya et al. 1982; Frank et al. 1983), they express only PKD2L1 (Huang et al. 2006; Ishimaru et al. 2006). Thus additional mechanisms for sour transduction are highly likely. If they are also expressed in Type III cells, then genetic ablation of the PKD2L1-expressing cells would eliminate these other mechanisms as well as the PKD2L1 channel itself. For example, Ugawa et al. (1998) and Ugawa (2003) reported that another candidate sour receptor, ASIC2, is also expressed in Type III cells although other investigators doubt the role of this channel in sour taste transduction in mice (Richter et al. 2004b).

The key event in transduction of acidic (sour-tasting) stimuli may not be the external pH, but rather internal acidification of the taste cell cytoplasm (Lyall et al. 2001; Richter et al. 2003). Richter et al. (2003) showed that when taste cells are acidified, only some respond with depolarization and a resulting rise in intracellular Ca^{++}. Because Type III taste cells are the only taste cells with voltage-gated Ca^{++} channels (Medler et al. 2003; DeFazio et al. 2006), these findings indicate that it is Type III cells that mediate sour taste transduction. If so, then ablation of Type III cells, as would be accomplished by using PKD2L1 promoter to drive toxin expression, should eliminate sour transduction regardless of what mechanism or receptor is actually involved.

Despite the loss of gustatory neural responses to sour in P2X2/P2X3 double knockout mice, the animals retain their ability to avoid sour-tasting substances in 2-bottle preference tests (Finger et al. 2005). These residual behavioral capabilities suggest that alternative, nongustatory means exist for the detection of ingested acidic solutions. Finger et al. (2005) suggested that solitary chemoreceptor cells of the larynx may contribute to this capability. Yet, we find no evidence for PKD2L1 expression in this cell population. Again, these results suggest alternative transduction mechanisms for "sour" tastants. One possibility is that acidic stimuli may be detected directly by intraepithelial oral nerve fibers because trigeminal fibers respond directly to application of citric acids (Pittman and Contreras 1998). Alternatively, acid-sensitive nerve fibers heavily innervate the larynx and epiglottis

(Smith and Hanamori 1991). These may be gustatory afferents as originally suggested by those investigators, or they may represent epithelial nerve fibers that are directly sensitive to acidification of the surrounding epithelium. If the latter, then they would be immune to knockout of the P2X receptors in taste buds and could account for the remaining avoidance of acidic stimuli in the P2X2/P2X3 double knockout mice (Finger et al. 2005).

In summary, our findings that PKD2L1 is expressed in Type III taste cells coupled with the genetic ablation studies of Huang et al (2006) carries 2 important implications for our understanding of the cellular organization of taste buds. In mice lacking PKD2L1-expressing (Type III) cells, detection of bitter, sweet, and umami qualities is unaffected. From this, we conclude that Type III cells are not required for transmission of taste information from Type II cells to the afferent nerves or else genetic ablation of the PKD2L1 cells would disrupt all taste transmission. Second, Type III cells cannot be obligatory precursors for the formation of Type II cells. Otherwise genetic ablation of the PKD2L1 cells would prevent the formation of Type II cells, again disrupting transduction of sweet, bitter, and umami qualities.

Supplementary Material

Supplementary material can be found at http://www.chemse.oxfordjournals.org.

Acknowledgements

The authors are grateful to Sue C. Kinnamon (Colorado State University) for important insights and conceptualizations presented in the discussion section of this paper. The authors thank Robert Margolskee (Mount Sinai School of Medicine and Howard Hughes Medical Institute, NY) for use of the TrpM5-GFP transgenic mice.

References

Bartel DL, Sullivan SL, Lavoie EG, Sevigny J, Finger TE. 2006. Nucleoside triphosphate diphosphohydrolase-2 is the ecto-ATPase of type I cells in taste buds. J Comp Neurol. 497:1–12.

Clapp TR, Medler KF, Damak S, Margolskee RF, Kinnamon SC. 2006. Mouse taste cells with G protein-coupled taste receptors lack voltage-gated calcium channels and SNAP-25. BMC Biol. 4:7.

Clapp TR, Stone LM, Margolskee RF, Kinnamon SC. 2001. Immunocytochemical evidence for co-expression of Type III IP3 receptor with signaling components of bitter taste transduction. BMC Neurosci. 2:6.

Crowley HH, Kinnamon JC. 1995. Transmission electron microscopy of gustatory epithelium. In: Spielman AI, Brand JG, editors. Experimental cell biology of taste and olfaction: current techniques and protocols. Boca Raton (FL): CRC Press. p. 105–114.

DeFazio RA, Dvoryanchikov G, Maruyama Y, Kim JW, Pereira E, Roper SD, Chaudhari N. 2006. Separate populations of receptor cells and presynaptic cells in mouse taste buds. J Neurosci. 26:3971–3980.

Delay RJ, Kinnamon JC, Roper SD. 1986. Ultrastructure of mouse vallate taste buds: II. Cell types and cell lineage. J Comp Neurol. 253:242–252.

Dvoryanchikov G, Tomchik SM, Chaudhari N. 2007. Biogenic amine synthesis and uptake in rodent taste buds. J Comp Neurol. 505:302–313.

Farbman AI, Hellekant G, Nelson A. 1985. Structure of taste buds in foliate papillae of the rhesus monkey, Macaca mulatta. Am J Anat. 172:41–56.

Finger TE, Danilova V, Barrows J, Bartel DL, Vigers AJ, Stone L, Hellekant G, Kinnamon SC. 2005. ATP signaling is crucial for communication from taste buds to gustatory nerves. Science. 310:1495–1499.

Finger TE, Simon SA. 2000. Cell biology of taste epithelium. In: Finger TE, Silver WL, Restrepo D, editors. Neurobiology of taste and smell. 2nd ed. New York: Wiley Press. p. 287–314.

Frank ME, Contreras RJ, Hettinger TP. 1983. Nerve fibers sensitive to ionic taste stimuli in chorda tympani of the rat. J Neurophysiol. 50:941–960.

Guagliardo NA, Hill DL. 2007. Fungiform taste bud degeneration in C57BL/6J mice following chorda-lingual nerve transection. J Comp Neurol. 504:206–216.

Hoon MA, Adler E, Lindemeier J, Battey JF, Ryba NJ, Zuker CS. 1999. Putative mammalian taste receptors: a class of taste-specific GPCRs with distinct topographic selectivity. Cell. 96:541–551.

Huang AL, Chen X, Hoon MA, Chandrashekar J, Guo W, Tränkner D, Ryba NJP, Zuker CS. 2006. The cells and logic for mammalian sour taste detection. Nature. 442:934–938.

Huang YJ, Maruyama Y, Dvoryanchikov G, Pereira E, Chaudhari N, Roper SD. 2007. The role of pannexin 1 hemichannels in ATP release and cell-cell communication in mouse taste buds. Proc Natl Acad Sci USA. 104:6436–6441.

Huesa G, van den Pol AN, Finger TE. 2005. Differential distribution of hypocretin (orexin) and melanin-concentrating hormone in the goldfish brain. J Comp Neurol. 488:476–491.

Ishimaru Y, Inada H, Kubota M, Zhuang H, Tominaga M, Matsunami H. 2006. Transient receptor potential family members PKD1L3 and PKD2L1 form a candidate sour taste receptor. Proc Natl Acad Sci USA. 103:12569–12574.

Kanazawa H, Yoshie S. 1996. The taste bud and its innervation in the rat as studied by immunohistochemistry for PGP 9.5. Arch Histol Cytol. 59:357–367.

Kaya N, Shen T, Lu SG, Zhao FL, Herness S. 2004. A paracrine signaling role for serotonin in rat taste buds: expression and localization of serotonin receptor subtypes. Am J Physiol Regul Integr Comp Physiol. 286:R649–R658.

Kim DJ, Roper SD. 1995. Localization of serotonin in taste buds: a comparative study in four vertebrates. J Comp Neurol. 353:364–370.

Kinnamon JC, Sherman TA, Roper SD. 1988. Ultrastructure of mouse vallate taste buds: III. Patterns of synaptic connectivity. J Comp Neurol. 270:1–10, 56–57.

Kinnamon JC, Taylor BJ, Delay RJ, Roper SD. 1985. Ultrastructure of mouse vallate taste buds. I. Taste cells and their associated synapses. J Comp Neurol. 235:48–60.

Lawton DM, Furness DN, Lindemann B, Hackney CM. 2000. Localization of the glutamate-aspartate transporter, GLAST, in rat taste buds. Eur J Neurosci. 12:3163–3171.

Lin W, Burks CA, Hansen DR, Kinnamon SC, Gilbertson TA. 2004. Taste receptor cells express pH-sensitive leak K$^+$ channels. J Neurophysiol. 92:2909–2919.

LopezJimenez ND, Cavenagh MM, Sainz E, Cruz-Ithier MA, Battey JF, Sullivan SL. 2006. Two members of the TRPP family of ion channels, Pkd1l3 and Pkd2l1, are co-expressed in a subset of taste receptor cells. J. Neurochem. 98:68–77.

Lyall V, Alam RI, Phan DQ, Ereso GL, Phan TH, Malik SA, Montrose MH, Chu S, Heck GL, Feldman GM, et al. 2001. Decrease in rat taste receptor cell intracellular pH is the proximate stimulus in sour taste transduction. Am J Physiol Cell Physiol. 281:C1005–C1013.

McLaughlin SK, McKinnon PJ, Margolskee RF. 1992. Gustducin is a taste-cell-specific G protein closely related to the transducins. Nature. 357:563–569.

Medler KF, Margolskee RF, Kinnamon SC. 2003. Electrophysiological characterization of voltage-gated currents in defined taste cell types of mice. J Neurosci. 23:2608–2617.

Miura H, Kato H, Kusakabe Y, Ninomiya Y, Hino A. 2005. Temporal changes in NCAM immunoreactivity during taste cell differentiation and cell lineage relationships in taste buds. Chem Senses. 30:367–375.

Miyoshi MA, Abe K, Emori Y. 2001. IP$_3$ receptor type 3 and PLCβ2 are co-expressed with taste receptors T1R and T2R in rat taste bud cells. Chem Senses. 26:259–265.

Murray RG. 1973. The ultrastructure of taste buds. In: Friedmann II, editor. Ultrastructure of sensory organs I. New York: American Elsevier. p. 1–81.

Murray RG. 1986. The mammalian taste bud type III cell: a critical analysis. J Ultrastruct Mol Struct Res. 95:175–88.

Nelson GM, Finger TE. 1993. Immunolocalization of different forms of neural cell adhesion molecule (NCAM) in rat taste buds. J Comp Neurol. 336:507–516.

Ninomiya Y, Tonosaki K, Funakoshi M. 1982. Gustatory neural response in the mouse. Brain Res. 244:370–373.

Perez CA, Huang L, Rong M, Kozak JA, Preuss AK, Zhang H, Max M, Margolskee RF. 2002. A transient receptor potential channel expressed in taste receptor cells. Nat Neurosci. 5:1169–1176.

Pittman DW, Contreras RJ. 1998. Responses of single lingual nerve fibers to thermal and chemical stimulation. Brain Res. 790:224–235.

Pumplin DW, Yu C, Smith DV. 1997. Light and dark cells of rat vallate taste buds are morphologically distinct cell types. J Comp Neurol. 378:389–410.

Richter TA, Caicedo A, Roper SD. 2003. Sour taste stimuli evoke Ca^{2+} and pH responses in mouse taste cells. J Physiol. 547:475–483.

Richter TA, Dvoryanchikov GA, Chaudhari N, Roper SD. 2004a. Acid-sensitive two-pore domain potassium (K2P) channels in mouse taste buds. J Neurophysiol. 92:1928–1936.

Richter TA, Dvoryanchikov GA, Roper SD, Chaudhari N. 2004b. Acid-sensing ion channel-2 is not necessary for sour taste in mice. J Neurosci. 24:4088–4091.

Romanov RA, Rogachevskaja OA, Bystrova MF, Jiang P, Margolskee RF, Kolesnikov SS. 2007. Afferent neurotransmission mediated by hemichannels in mammalian taste cells. EMBO J. 26:657–667.

Roper SD. 2006. Cell communication in taste buds. Cell Mol Life Sci. 63:1494–1500.

Rössler P, Kroner C, Freitag J, Noè J, Breer H. 1998. Identification of a phospholipase C beta subtype in rat taste cells. Eur J Cell Biol. 77:253–261.

Smith DV, Hanamori T. 1991. Organization of gustatory sensitivities in hamster superior laryngeal nerve fibers. J Neurophysiol. 65:1098–1114.

Stevens DR, Seifert R, Bufe B, Muller F, Kremmer E, Gauss R, Meyerhof W, Kaupp UB, Lindemann B. 2001. Hyperpolarization-activated channels HCN1 and HCN4 mediate responses to sour stimuli. Nature. 413:631–635.

Takeda M. 1976. An electron microscopic study on the innervation in the taste buds of the mouse circumvallate papillae. Arch Histol Jpn. 39:257–269.

Takeda M. 1977. Uptake of 5-hydroxytryptophan by gustatory cells in the mouse taste bud. Arch Histol Jpn. 40:243–250.

Takeda M, Hoshino T. 1975. Fine structure of taste buds in the rat. Arch Histol Jpn. 37:395–413.

Takeda M, Shishido Y, Kitao K, Suzuki Y. 1981. Biogenic monoamines in developing taste buds of mouse circumvallate papillae. Arch Histol Jpn. 44:485–495.

Takeda M, Suzuki Y, Obara N, Nagai Y. 1992. Neural cell adhesion molecule of taste buds. J Electron Microsc (Tokyo). 41:375–380.

Ugawa S. 2003. Identification of sour-taste receptor genes. Anat Sci Int. 78:205–210.

Ugawa S, Minami Y, Guo W, Saishin Y, Takatsuji K, Yamamoto T, Tohyama M, Shimada S. 1998. Receptor that leaves a sour taste in the mouth. Nature. 395:555–556.

Voets T, Talavera K, Owsianik G, Nilius B. 2005. Sensing with TRP channels. Nat Chem Biol. 1:85–92.

Yang R, Ma H, Thomas SM, Kinnamon JC. 2007. Immunocytochemical analysis of syntaxin-1 in rat circumvallate taste buds. J Comp Neurol. 502:883–893.

Yang R, Stoick CL, Kinnamon JC. 2004. Synaptobrevin-2-like immunoreactivity is associated with vesicles at synapses in rat circumvallate taste buds. J Comp Neurol. 471:59–71.

Yang R, Tabata S, Crowley HH, Margolskee RF, Kinnamon JC. 2000. Ultrastructural localization of gustducin immunoreactivity in microvilli of type II taste cells in the rat. J Comp Neurol. 425:139–151.

Yee CL, Jones KR, Finger TE. 2003. Brain-derived neurotropic factor is present in adult mouse taste cells with synapse. J Comp Neurol. 459:15–24.

Yee CL, Yang R, Bottger B, Finger TE, Kinnamon JC. 2001. "Type III" cells of rat taste buds: immunohistochemical and ultrastructural studies of neuron-specific enolase, protein gene product 9.5, and serotonin. J Comp Neurol. 440:97–108.

Yoshie S, Wakasugi C, Teraki Y, Fujita T. 1990. Fine structure of the taste bud in guinea pigs. I. Cell characterization and innervation patterns. Arch Histol Cytol. 53:103–119.

Zhang Y, Hoon MA, Chandrashekar J, Mueller KL, Cook B, Wu D, Zuker CS, Ryba NJP. 2003. Coding of sweet, bitter, and umami tastes: different receptor cells sharing similar signaling pathways. Cell. 112:293–301.